Analysis of Worst-Case Hot-Carrier Conditions for n-type MOSFET

Ivan Starkov and Hajdin Ceric
CDL for Reliability Issues in Microelectronics
at the Institute for Microelectronics, TU Wien
Gußhausstraße 27-29, A-1040 Wien, Austria
Email: starkov@iue.tiwien.ac.at

Stanislav Tyaginov and Tibor Grasser
Institute for Microelectronics, TU Wien
Gußhausstraße 27-29, A-1040 Wien, Austria
Email: tyaginov@iue.tiwien.ac.at

***Abstract*—We analyze the worst-case conditions of hot-carrier induced degradation with our model which is based on the evaluation of the carrier distribution function along the $\mathbf{Si/SiO_2}$ interface, i.e. thorough consideration of carrier transport. The distribution function obtained by means of a full-band Monte-Carlo device simulator is used to calculate the acceleration integral, which controls how effectively the carriers are breaking Si-H bonds. Therefore, we analyze these worst-case conditions using this integral as a criterion. We compare the numerical picture with the experimental one and conclude that the model fits the experimental data rather accurately and confirm that these conditions correspond to the relation $V_{\mathrm{gs}} = 0.4V_{\mathrm{ds}}$ between gate and drain voltages. The simplified treatment of carrier transport using the non-Maxwellian but still analytical distribution function is also discussed. A discrepancy between experimental results and simulations, which occurred while employing this simplified approach, is shown and explained.**

***Index Terms*—hot-carrier degradation, TCAD, MOSFET, worst-case conditions, distribution function.**

I. Introduction

The worst-case conditions (WCC) of hot-carrier degradation (HCD) in the case of a long-channel n-MOSFET are reached when the substrate current I_{sub} is at its maximum [1]–[8]. For long-channel transistors the silicon-hydrogen bond-breakage process is dominantly triggered by the interaction of the bond with a solitary carrier. This carrier is accelerated by the electric field up to energies sufficient enough to effectively rupture the bond in a single collision. Since impact ionization is a process which has an analogous activation nature, the concentration of electron-hole pairs generated by impact ionization may be used as a criterion how hot are the carriers. As a consequence, one may judge about the degradation intensity on the substrate current I_{sub} which is composed of majority carriers generated by impact ionization [5], [6], [8]. Usually the I_{sub} maximum is observed when $V_{\mathrm{gs}} = (0.4-0.5)V_{\mathrm{ds}}$ and, hence, it is assumed that the most severe degradation corresponds to these stress conditions.

However, impact ionization and bond-breakage are different processes characterized by various values of parameters, such as reaction cross sections and activation energies [9]–[12]. Therefore, impact ionization does not necessarily play a role of measure how intensive HCD is. The bond-breakage process is controlled by the carrier acceleration integral (AI) which weights the intensity of the dissociation process induced by a high-energetic carrier with the probability to find such a carrier [12], [13]. Since the AI includes the reaction cross section, this quantity better reflects the intensity of the interface state generation. In this work we apply our approach for hot-carrier degradation modeling [12], [13] in order to describe the worst-case conditions of HCD. The model is based on thorough treatment of carrier transport using a full-band Monte-Carlo device simulator which solves the Boltzmann transport equation and allows for a calculation of the carrier distribution function (DF) at any position of the device for a particular device geometry and stress conditions. Since the Monte-Carlo method is very time-consuming we undertake an attempt to substitute the precise carrier transport module by a simplified treatment, i.e. use an analytical form of a non-Maxwellian distribution function proposed by Fiegna *et al.* [14] and well applicable for long-channel devices [14], [15]. We analyze also discrepancy between these two approaches and conclude on the limitations of the simplified version of the model.

II. Experimental support

5V n-MOSFETs fabricated on a standard $0.35\ \mu\mathrm{m}$ CMOS have been stressed at a series of gate voltages $V_{\mathrm{gs}} = 2.0, 2.5, 2.8\mathrm{V}$ and the fixed drain voltage of $V_{\mathrm{ds}} = 6.5\mathrm{V}$ for $10^4\mathrm{s}$ at an ambient temperature of 25°C. The device architecture is sketched in Fig. 1 as well the net doping profile. The device channel length is $0.5\ \mu\mathrm{m}$. Together with a relatively high operation voltage this channel length ensures that the single-electron mechanism of the Si-H bond dissociation is the dominating one [6].

III. The approach

Our model considers two components of the Si-H bond dissociation process, i.e. the single-carrier and multiple-carrier mechanisms (SC- and MC-modes) [12], [13]. As we showed in our previous work, even in the case of a relatively high-voltage device the second mechanism provides a considerable contribution to the total damage and thus must not be omitted [12]. Both components are controlled by the carrier acceleration integral:

$$I_{\mathrm{SC/MC}} = \nu_{\mathrm{SC/MC}} \int_{E_{\mathrm{th}}}^{\infty} f(E)g(E)\sigma_{\mathrm{SC/MC}}(E)v(E)dE, \quad (1)$$

978-1-4244-9136-0/11/$26.00 ©2011 IEEE

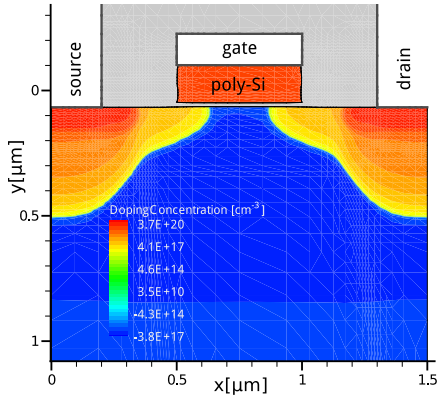

Fig. 1. The topology of n-MOS with the net doping profile represented by the color map.

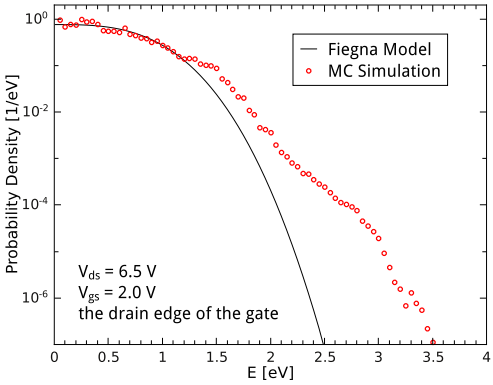

Fig. 2. The carrier distribution function: the result of Monte-Carlo simulations and its fitting with the Fiegna model.

where $f(E)$ is the carrier DF calculated employing full-band Monte-Carlo device simulator MONJU [16], $g(E)$ the density-of-states while $\sigma_{\mathrm{SC/MC}}$ is the reaction cross section for the dissociation process. The carrier velocity is designated as $v(E)$ and integration is performed starting from the threshold energy E_{th}.

As we discussed in [12], [17] the dose of damage provided by the MC-component is homogeneously distributed over the lateral coordinate. This is because the prefactor in the MC-induced interface state concentration (see [12], [17]) defined by the acceleration integral is already saturated due to the high concentration of relatively "cold" carriers (represented by the low-energy fragment of the DF). As a result, the non-uniform nature of HCD is related to the single-carrier bond-breakage process with the corresponding contribution to the total interface state density N_{it} localized near the drain end of the gate. Therefore, in order to find the stress conditions corresponding to the worst-case scenario, we suggest to analyze the behavior of the acceleration integral, not considering the interaction between the SC and MC-mechanisms. In literature, one may find other criteria how efficiently carriers interact with the bond, i.e. the maximum of the electric field, the carrier dynamic temperature, position where the DF demonstrates most extended high-energy tales, etc. However, as we showed in [13], the N_{it} peak just corresponds to the maximum of the AI and is shifted away with respect to maxima of other quantities.

In order to create the numerical picture for the worst-case conditions the following computational procedure was used. Initially, we varied both V_{ds} and V_{gs} voltages in the range of 0...6.0 V. Afterwards, for each pair V_{ds},V_{gs} we calculated the set of the carrier DFs, i.e. distribution functions at each point on the Si/SiO_2 interface. This information was used to calculate the dependences of the carrier acceleration integral vs. the lateral coordinate. After processing these dependencies we have plotted the maximum value of the acceleration integral I_{SC} as a function of V_{ds},V_{gs}. These three-dimensional plots (discussed in details in the next Section) have been further compared with experimental results and analyzed.

Although the distribution function obtained by a direct solution of the Boltzmann transport equation better represents the matter, Monte-Carlo simulations are usually extremely time-consuming. As a result, in commercial TCAD simulators simplified treatments of carrier transport are used. Among them are the drift-diffusion and energy transport schemes, see e.g. [18]. One of the most popular approaches which employs an analytical expression for non-Maxwellian distribution functions is the Fiegna model [14], [15]. This model is applicable for devices with a channel length longer than 0.5 μm. which is just suitable for our case.

Within this approach the following expression for the DF is proposed:

$$f_{\mathrm{Fi}}(E) = C \exp\left(-\frac{\chi E^3}{|F|^{1.5}}\right), \qquad (2)$$

where C denotes the normalization constant, F represents the applied electric field and χ is a fitting parameter. This parameter may be adjusted in order to represent the real distribution function at a certain point. The choice of this point may substantially affect all the results. In our work the value of χ was found in a way guaranteeing a minimal discrepancy between experimental and simulated charts $I_{\mathrm{SC}}(V_{\mathrm{ds}}, V_{\mathrm{gs}})$.

Explicitly, the value of χ used in this work is $1.62\cdot 10^8$ $\mathrm{eV}^{-3}\mathrm{V}^{1.5}\mathrm{cm}^{-1.5}$ (note that values reported in papers [14] and [15] are $1.3\cdot 10^8$ and $0.8\cdot 10^8$ $\mathrm{eV}^{-3}\mathrm{V}^{1.5}\mathrm{cm}^{-1.5}$, respectively). This parameter was found while fitting the distribution function at the drain end of the gate by the Fiegna expression, see Fig. 2. The most significant discrepancy between these distribution functions is observed at higher energies. This circumstance suggests that the acceleration integrals calculated using these two different DFs should strongly diverge under conditions corresponding to the most extended high-energy tails of the distribution function.

IV. Results

The measured substrate current as a function of stress drain and gate voltages is depicted in Fig. 3. Fig. 4 demonstrates the maximum value of the acceleration integral I_{SC} plotted

vs. $V_{\rm ds}$ and $V_{\rm gs}$ and calculated within our HCD model which is based on the direct solution of the Boltzmann transport equation. Fig. 5 demonstrated the same as Fig. 4 but the AI was calculated employing the fitting function $f_{\rm Fi}(E)$. A comparison of these figures allows us to make several conclusions. First of all, our Monte-Carlo based HCD model provides a very good agreement between the experiment and theory. In contrast, the simplified version which employs the Fiegna function instead of the real DF, fails in the area of low $V_{\rm gs}$ with high $V_{\rm ds}$. This is because at high $V_{\rm ds}$ the electric field still reaches high values and thus results in enormously pronounced high-energy tails of $f_{\rm Fi}(E)$. In practice this regime is characterized by a low $I_{\rm dlin}$ and thus degradation is weak (this trend is pronounced in Fig. 4). In other words, if $V_{\rm ds}$ is fixed and $V_{\rm gs}$ varies, the substrate current first grows, reaches its maximum and then decreases. This tendency is also supported by Fig. 6 (the data are extracted from Fig. 3) where $V_{\rm gs}$ is presented as a function of $V_{\rm ds}$ which is found as the value guaranteeing the maximum of either $I_{\rm sub}$ (experimental data) or $I_{\rm SC}$ (simulations with our HCD model) for the chosen value of $V_{\rm ds}$. However, according to predictions of Fig. 5 the maximum degradation dose monotonously increases with $V_{\rm gs}$.

For a drain voltage above 2.0V, $V_{\rm ds}$ and $V_{\rm gs}$ corresponding to the WCC are linked by the relationship $V_{\rm gs} = 0.4V_{\rm ds}$ and this tendency is supported by our HCD model (Fig. 6). This trend is also confirmed in Fig. 7 where the linear drain current $I_{\rm dlin}$ degradation is plotted vs. the stress time for various $V_{\rm gs}$ of 2.0, 2.5 and 2.8 V while $V_{\rm ds}$ is fixed at 6.5 V. The maximum in the substrate current is usually explained as a trade-off between two competing tendencies: the increase of the drain current due to the $V_{\rm gs}$ growth and the decrease of impact ionization intensity due to the lateral field weakening, see [19]. At the same time for low $V_{\rm ds} < 1.0V$ the device operates in a regime far away from saturation and thus the second tendency does not occur. Therefore, in this range $I_{\rm sub}$ grows with $V_{\rm gs}$. This behavior is reflected in Fig. 6 (the left branch of the curve) where the reduction in $V_{\rm ds}$ is compensated by an increase in $V_{\rm gs}$. In other words, in the case of low $V_{\rm ds}$ carriers are accelerated by the gate bias which plays the dominant role.

Finally, we plotted the position of the most severe degradation spot as a function of the stress voltages (Fig. 8). As we previously showed [13], just the maximum of the acceleration integral (not of other quantities such as the electric field, average carrier energy, etc) determines the position of the $N_{\rm it}$ peak. Therefore, this graph can be used to predict where the most degraded section of the device is located. Note that this color map reflects the pattern shown in Fig. 4: e.g. the orange area pronounced in Fig. 4 (and bordered by the right contour curve) corresponds to the light green spot from Fig. 8.

V. Conclusion

We have examined the worst-case conditions of hot-carrier degradation in the case of 5V n-MOSFETs. For this purpose we employed our HCD model which is based on a thorough treatment of the carrier distribution function obtained using a full-band Monte-Carlo device simulator. We also employed

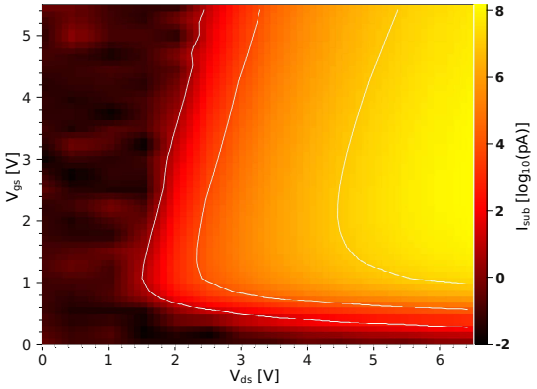

Fig. 3. The substrate current as a function of $V_{\rm ds}$,$V_{\rm gs}$.

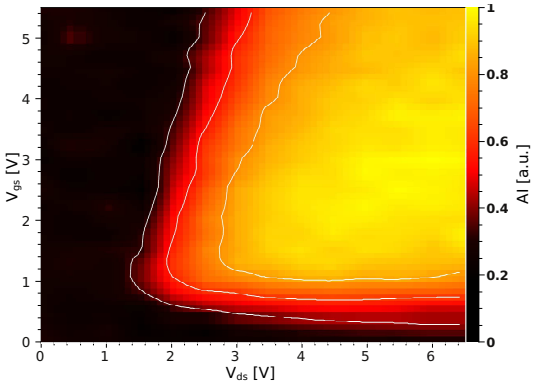

Fig. 4. The maximum value of the acceleration integral as a function of $V_{\rm ds}$,$V_{\rm gs}$ calculated using the thorough solution of the Boltzmann transport equation.

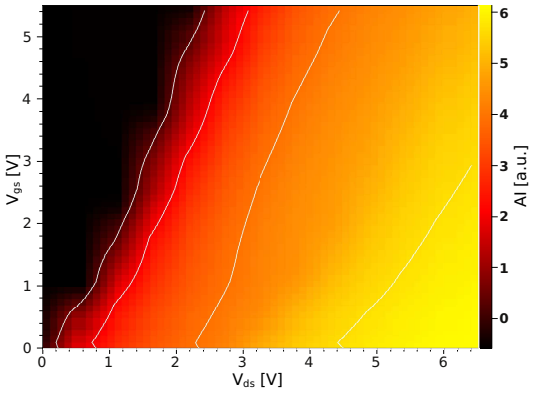

Fig. 5. The maximum value of the acceleration integral as a function of $V_{\rm ds}$,$V_{\rm gs}$ calculated with the Fiegna model.

a simplified treatment of carrier transport with the Fiegna model which was reported as applicable for device channel lengths greater than $0.5\ \mu$m which is the case for our devices. Since the degradation is controlled by the carrier acceleration integral, this quantity was plotted against $V_{\rm ds}$ and $V_{\rm gs}$ and compared with the experimental map $I_{\rm sub}(V_{\rm ds}, V_{\rm gs})$. We have concluded that our model represents the WCC with a reasonable accuracy. For instance, the relation of $V_{\rm gs} = 0.4V_{\rm ds}$ typical for the WCC was reproduced. As for the Fiegna model, it fails in the case of low $V_{\rm gs}$ and high $V_{\rm ds}$ and cannot be

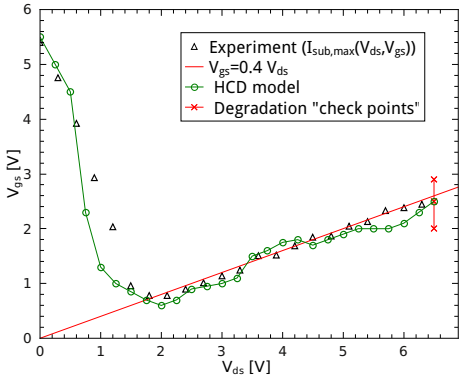

Fig. 6. The gate voltage as a function of the drain voltage corresponding to the worst-case conditions.

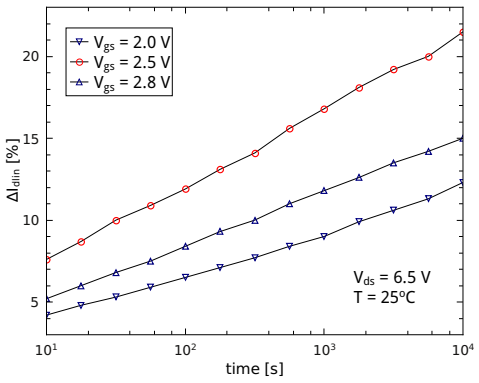

Fig. 7. Degradation of I_{dlin} for several stress gate voltages and the fixed drain voltage.

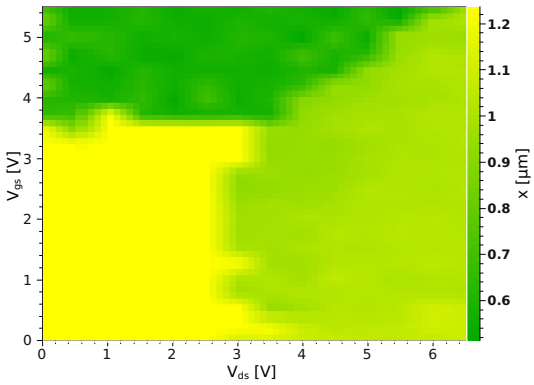

Fig. 8. The position of the maximum acceleration integral as a function of V_{ds},V_{gs}. The graph is calculated with our HCD model.

used for proper HCD modeling. Finally, our HCD model predicts the position where the most severe degradation dose is localized (i.e. between the drain end of the gate and the drain).

Acknowledgment

The authors would like to thank Dr. Hubert Enichlmair and Dr. Jong Mun Park from the Process Development and Implementation Department, Austriamicrosystems AG for presented experimental data. We also very much appreciate stimulating discussions with Prof. Christoph Jungemann (Institute for Microelectronics and Circuit Theory, Bundeswehr University, München,) and his support with the Monte-Carlo device simulator MONJU. This work has received funding from the EC's FP7 grant agreement n°216436 (ATHENIS) and from the ENIAC MODERN project n°820379.

References

[1] S. Rauch, F. Guarin, and G. La Rosa, "Impact of E-E scattering to the hot carrier degradation of deep submicron nMOSFETs," *IEEE Electron Dev. Lett.*, vol. 19, no. 12, pp. 463–465, 1998.

[2] D. Brisbin, P. Lindorfer, and P. Chaparala, "Substrate current independent hot carrier degradation in nLDMOS devices," in *Proc. International Reliability Physics Symposium (IRPS)*, 2006, pp. 329–333.

[3] M. Annese, S. Carniello, and S.Manzini, "Design and optimization of a hot-carrier resistant high-voltage nMOS transistor," *IEEE Trans. Electron Dev.*, vol. 52, no. 7, pp. 1634–1639, 2005.

[4] P. Santos, H. Quaresma, A. Silva, and M. Lanca, "High-voltage nMOS design in fully implanted twin-well CMOS," *Microel. Jour.*, vol. 35, no. 9, pp. 723–730, 2004.

[5] S. Rauch and G. L. Rosa, "CMOS hot carrier: From physics to end of life projections, and qualification," in *Proc. International Reliability Physics Symposium (IRPS), tutorial*, 2010.

[6] A. Bravaix and V. Huard, "Hot-carrier degradation issues in advanced CMOS nodes," in *Proc. European Symposium on Reliability of Electron Devices Failure Physics and Analysis (ESREF), tutorial*, 2010.

[7] M. Song, K. MacWilliams, and C. Woo, "Comparison of nMOS and pMOS hot carrier effects from 300 to 77K," *IEEE Trans Electron Dev.*, vol. 44, no. 2, pp. 268–276, 1997.

[8] J. Wang-Ratkovic, R. Lacoe, K. Williams, M. Song, S. Brown, and G. Yabiku, "New understanding of LDD CMOS hot-carrier degradation and device lifetime at cryogenic temperatures," *International Reliability Physics Symposium*, pp. 312–314, 2003.

[9] K. Hess, A. Haggag, W. McMahon, K. Cheng, J. Lee, and J. Lyding, "The physics of determining chip reliability," *Circuits and Devices Mag.*, pp. 33–38, 2001.

[10] C. Guerin, V. Huard, and A. Bravaix, "General framework about defect creation at the Si/SiO_2 interface," *Journ. Appl. Phys.*, vol. 105, no. 114513, 2009.

[11] A. Bravaix, C. Guerin, V. Huard, D. Roy, J. Roux, and E. Vincent, "Hot-carrier acceleration factors for low power management in DC-AC stressed 40nm nMOS node at high temperature," in *Proc. International Reliability Physics Symposium (IRPS)*, 2009, pp. 531–546.

[12] S. Tyaginov, I. Starkov, O. Triebl, J. Cervenka, C. Jungemann, S. Carniello, J. Park, H. Enichlmail, C. Kernstock, E. Seebacher, R. Minixhofer, H. Ceric, and T. Grasser, "Interface traps density-of-states as a vital component for hot-carrier degradation modeling," *Microel. Reliab.*, vol. 50, pp. 1267–1272, 2010.

[13] I. Starkov, S. Tyaginov, H. Enichlmair, J. Cervenka, C. Jungemann, S. Carniello, J. Park, H. Ceric, and T. Grasser, "Hot-carrier degradation caused interface state profile - simulations vs. experiment," *Journal of Vacuum Science and Technology - B*, vol. 29, no. 1, pp. 01AB09–1–01AB09–8, 2011.

[14] C. Fiegna, F. Venturi, M. Melanotte, E. Sangiorgi, and B. Ricco, "Simple and efficient modeling of EPROM writing," *IEEE Trans Electron Dev.*, vol. 38, no. 3, pp. 603–610, 1991.

[15] A. Zaka, Q. Rafhay, M. Iellina, P. Palestri, R. Clerc, D. Rideau, D. Garetto, J. Singer, G. Pananakakis, C. Tavernier, and H. Jaouen, "On the accuracy of current TCAD hot carrier injection models in nanoscale devices," *Solid-State Electron.*, vol. in press, 2010.

[16] C. Jungemann and B. Meinerzhagen, *Hierarchical Device Simulation*. Springer Verlag Wien/New York, 2003.

[17] S. Tyaginov, I. Starkov, O. Triebl, J. Cervenka, C. Jungemann, S. Carniello, J. Park, H. Enichlmair, M. Karner, C. Kernstock, E. Seebacher, R. Minixhofer, H. Ceric, and T. Grasser, "Hot-carrier degradation modeling using full-band monte-carlo simulations," in *Proc. International Symposium on the Physical & Failure Analysis of Integrated Circuits (IPFA)*, 2010.

[18] *DESSIS ISE TCAD Manual Release 9.0*, 2002.

[19] S. Sze and K. Ng, *Physics of semiconductor devices*, ser. Wiley-Interscience publication. Wiley-Interscience, 2007.